

Study of differentially expressed genes related to plant height and yield in two alfalfa cultivars based on RNA-seq

Jiangjiao Qi¹, Xue Yu¹, Xuzhe Wang¹, Fanfan Zhang¹, Chunhui Ma^{Corresp. 1}

¹ College of Animal Science & Technology, Shihezi University, Shihezi, Xinjiang, China

Corresponding Author: Chunhui Ma
Email address: chunhuima@126.com

Background. Alfalfa (*Medicago sativa* L.) is a kind of forage with high relative feeding value in farming and livestock breeding, and is of great significance to the development of animal husbandry. The rapid growth of the aboveground part of alfalfa is the main factors limiting crop yield. Clarifying the molecular mechanisms that regulate alfalfa vigorous-growing may contribute to the development of molecular breeding for alfalfa. This mechanism, however, has not been extensively studied for alfalfa.

Methods. In the present study, the phenotypes of five alfalfa cultivars were evaluated. We found that the rapid growth of stems significantly affected plant height and yield of tall-type alfalfa (WL 712) and low-type alfalfa (Aohan). The vigorous-growing WL712 and slow-growing Aohan exhibited significantly different plant heights, stem diameters and internode lengths. RNA-seq was performed on the stems of both cultivars. GO enrichment analysis was conducted on all differentially expressed genes (DEGs).

Result. In WL712 alfalfa cultivar, we found that seven DEG groups were found to be involved in the formation of water-conducting tissue in vascular plants, biosynthesis and degradation of lignin, formation of the primary or secondary cell wall, cell enlargement and plant growth, cell division and shoot initiation, stem growth and induced germination, and cell elongation. KEGG analysis showed that plant hormone signal transduction, photosynthesis, and phenylpropanoid biosynthesis regulated the rapid growth of stems. Members of the *WRKY* family related to plant growth and development. Members of the *NAC* and *MYB* gene families related to the synthesis of cellulose and hemicellulose, and the development of secondary cell wall fibres. Some *MYB* family members act as activators or inhibitors and are involved in plant growth regulation. Our research results not only enrich the transcriptome database of alfalfa, but also provide valuable information for explaining the molecular mechanism of fast-growing, and can provide reference for the actual production of alfalfa at the same latitude and similar soil in the world.

Study of differentially expressed genes related to plant height and yield in two alfalfa cultivars based on RNA-seq

Jiangjiao Qi, Yuxue, Xuzhe Wang, Fanfan Zhang and Chunhui Ma

College of Animal Science & Technology, Shihezi University, Shihezi, 832003, Xinjiang, China

Corresponding Author:

Chunhui Ma

Shihezi University, Shihezi, 832003, Xinjiang, China

E-mails: chunhuima@126.com

Abstract

Background. Alfalfa (*Medicago sativa* L.) is a kind of forage with high relative feeding value in farming and livestock breeding, and is of great significance to the development of animal husbandry. The rapid growth of the aboveground part of alfalfa is the main factors limiting crop yield. Clarifying the molecular mechanisms that regulate alfalfa vigorous-growing may contribute to the development of molecular breeding for alfalfa. This mechanism, however, has not been extensively studied for alfalfa.

Methods. In the present study, the phenotypes of five alfalfa cultivars were evaluated. We found that the rapid growth of stems significantly affected plant height and yield of tall-type alfalfa (WL 712) and low-type alfalfa (Aohan). The vigorous-growing WL712 and slow-growing Aohan exhibited significantly different plant heights, stem diameters and internode lengths. RNA-seq was performed on the stems of both cultivars. GO enrichment analysis was conducted on all differentially expressed genes (DEGs).

Result. In WL 712 alfalfa cultivar, we found that seven DEG groups were found to be involved in the formation of water-conducting tissue in vascular plants, biosynthesis and degradation of lignin, formation of the primary or secondary cell wall, cell enlargement and plant growth, cell division and shoot initiation, stem growth and induced germination, and cell elongation. KEGG analysis showed that plant hormone signal transduction, photosynthesis, and phenylpropanoid biosynthesis regulated the rapid growth of stems. Members of the *WRKY* family related to plant growth and development. Members of the *NAC* and *MYB* gene families related to the synthesis of cellulose and hemicellulose, and the development of secondary cell wall fibres. Some *MYB* family members act as activators or inhibitors and are involved in plant growth regulation. Our research results not only enrich the transcriptome database of alfalfa, but also provide valuable information for explaining the molecular mechanism of fast-growing, and can provide reference for the actual production of alfalfa at the same latitude and similar soil in the world.

Key words: *Medicago sativa*, RNA – seq, DEGs, Stem elongation, Vigorous-growing, Slow-growing

40

41

42 Introduction

43 The stem is an important vegetative organ between the root and leaf of a plant and transports
44 nutrients and water (Ernest et al., 2020). The stems of alfalfa also play a role in photosynthesis,
45 nutrient storage, and regeneration (Sena, 2014). In the process of stem growth and development,
46 stem tips grow continuously, whereas branches, leaves, and lateral branches are produced
47 successively, which together constitute a huge branch system (Yu et al., 2015; Jaykumar &
48 Mahendra, 2016). The degree of stem development is closely related to the life cycle of plants
49 (Sophia et al., 2021), especially the aboveground biomass of the plant (Kleyer et al., 2019). Alfalfa,
50 with stems and branches as the main components of grass yield, is a typical representative crop.

51 Alfalfa is a feed crop with a high economic value (Kumar et al., 2018). In addition to its stress
52 resistance properties, it has been the focus of research because of its perennial nature and high
53 nutritional value (Wang et al., 2017; Diatta, Doohong & Jagadish, 2021). The stems and leaves of
54 alfalfa have the highest nutrient content and are the main parts areas of animal forage (Sulc et al.,
55 2021). Owing to the cross-pollination of alfalfa, most cultivars have a complex genetic
56 background. Restricted by its genetic characteristics, growth performance and nutritional quality
57 are uneven (Bambang et al., 2021). Alfalfa stalks are composed of nodes and internodes, which
58 affect plant height and yield. The height and stem diameter of alfalfa are important factors that
59 restrict its biomass (Monirifar, 2011). Therefore, increasing the number of alfalfa vegetative
60 branches, vegetative growth time, and delaying the flowering time of plants are crucial for
61 improving the nutritional quality and yield of forage grass (Aung et al., 2015), ~~which is also one~~
62 ~~of the hot spots that breeders pay attention to at this stage.~~ Previous studies have reported
63 significant differences in alfalfa plant height and hay yield (Ziliotto et al., 2010). The WL alfalfa
64 series exhibited the best growth performance when compared to different alfalfa cultivars (Tetteh
65 & Bonsu, 1997). Plant spacing and light significantly effect on alfalfa forage yield and weed
66 inhibition in the field (Celebi et al., 2010). Compound fertilizers can increase the nutrient content
67 of soil and improve the yield of alfalfa (Iryna, Rudra & Doohong, 2021; Na et al., 2021).
68 Additionally, the growth and development periods of alfalfa are equally important for its yield
69 (Martin et al., 2010). During the growth of alfalfa, the budding stage that has excellent nutritional
70 quality and grass yield has always been a hot period of concern for breeders around the world (Fan
71 et al., 2018). Currently, research on the growth performance of alfalfa mainly focuses on the
72 physiological level. Few reports have revealed the molecular mechanism of alfalfa stem elongation
73 and diameter enlargement and its effect on biomass at the gene level.

74 Owing to the lack of a complete reference genome sequence, previous studies on the stress-
75 response genes of alfalfa have used nonparametric transcriptome analysis (Yuan et al., 2020; Wang
76 et al., 2021; Gao et al., 2016; Arshad, Gruber & Hannoufa et al., 2018). Reference-free
77 transcriptome refers to the sequencing of eukaryotic transcriptomes in the absence of a reference
78 genome. After obtaining the original data for eukaryotic nonparametric transcriptome sequencing,
79 the quality control splicing is first ~~performed into~~ unigene, and then ~~the unigene is used~~ as the

80 reference sequence for subsequent analysis. However, with the availability of whole-genome
81 sequencing and annotation of alfalfa (Zhongmu 1), studying the alfalfa genome has become easier
82 (Zhang et al., 2021). Transcriptome sequencing is the study of all mRNAs ~~transcribed by a specific~~
83 ~~tissue in a certain period~~, which is the basis for the study of gene function and is important for
84 understanding the development of organisms (Wang, Gerstein & Snyder, 2009). With the
85 advantages of high-throughput, high accuracy, and high sensitivity, RNA-seq can be used to study
86 changes in the expression level of transcripts ~~in vivo~~ to understand or reveal the intrinsic
87 relationship between gene expression and biological phenotypes (Guo et al., 2021). At present,
88 RNA-seq technology has become a common method to study the growth and development of ~~rice,~~
89 ~~Arabidopsis thaliana, upland cotton and wheat~~ (Chen et al., 2020; Kim et al., 2021; Zheng et al.,
90 2021). Next-generation high-throughput sequencing technology can be used to comprehensively
91 obtain the transcript information of alfalfa and screen out the significantly different genes related
92 to stem elongation and diameter enlargement.

93 **The fast-growing** of alfalfa is a important factor of alfalfa that ~~can~~ affect plant height and
94 yield (Yan et al., 2021). Exploring the molecular mechanisms of **vigorous-growing of alfalfa** may
95 be helpful to improve the yield ~~of alfalfa cultivars~~. The application of gene editing technology may
96 be more efficient than traditional techniques such as cross-breeding. We identified differentially
97 expressed genes (DEGs) in the stem of alfalfa "WL712" (USA, **FDC = 10.2**) and "Aohan" (China,
98 FDC = 2.0) using RNA-seq, further identified the key genes regulating vigorous-growing of alfalfa
99 by bioinformatics analysis and predicted their functions. These results may be helpful in clarifying
100 the molecular mechanism of **vigorous-growing of alfalfa**, establishing a regulatory network of the
101 growth and development of dominant cultivars, and laying a theoretical foundation for molecular
102 breeding and the introduction of dominant cultivars.

103 **Materials & Methods**

104 **Characterisation of phenotypic traits**

105 Five cultivars of alfalfa (WL 712, Victoria, Kangsai, Knight 2, and Aohan) were planted at
106 the experimental herbage station of Shihezi University, Xinjiang, China (N44 ° 20 ', E88 ° 30',
107 altitude 420 m) (**Table S1a**). Its characteristic is temperate continental arid climate, with an
108 average annual temperature of 8.1°C. Before planting, we adopted the "S" shaped sampling
109 method, and nine soil samples were obtained. the nutrient status of the soil (20 cm) was as follows:
110 available nitrogen 92.6 mg/kg, organic matter 12.4 g/kg, available potassium 168.5 mg/kg,
111 available phosphorus 33.2 mg/kg, and pH 7.26 (**Table S1b**).

112 In June 2019 and 2020, alfalfa was planted in a 40 m² plot using a completely randomised
113 design. To ensure consistency among the cultivars, thirty-six stems with well-growing single
114 alfalfa were collected from each cultivar. Single-row planting method with sampling plant spacing
115 of 40 cm and row spacing of 60 cm, with three biological replicates per cultivar. At the budding
116 stage, agronomic traits of five randomly selected plants were determined from each of the three
117 biological replicates. The absolute distance from the root to the top of the main stem was calculated
118 as plant height using ruler. ~~This counting method calculates the~~ number of branches and nodes.
119 The stem diameter and internode length were ~~calculated~~ using calipers. The leaf area was measured


120 using leaf area meter. Five plants in each row were randomly selected and weighed, and the
121 average value was calculated as the total fresh weight per plant. By comparing and analyzing the
122 growth indexes of different varieties, it was finally determined that WL712 represented a vigorous
123 and fast-growing variety and Aohan represented a short and slow-growing variety (**Fig. S1**).

124 **Cultivation of experimental materials and sample collection**

125 Stems ~~with vigorous-growing~~ WL712 and ~~slow-growing~~ Aohan were collected and cut into
126 8 cm pieces, leaving an axillary bud. The ~~plant~~ were cultivated on cutting beds in the greenhouse
127 (light/dark: 16 h / 8 h, Temp: 25 °C / 20 °C, humidity 70%) of the Beiyuan campus of Shihezi
128 University for 20 days, and surviving plants were transplanted into plastic pots (diameter 32 cm,
129 height 35 cm). Nutrient soil: vermiculite = 1: 1 (cultivation and management methods were
130 consistent). More than 30 individual plants of both WL712 and Aohan survived in the
131 greenhouse. Five plants of ~~fast-growing~~ WL712 and ~~slow-growing~~ Aohan alfalfa were randomly
132 selected, ~~respectively~~, and the plant height, internode length, stem diameter, leaf area and yield
133 were determined.

134 At the budding stage, stems (approximately 1.5 cm) of each cultivar were collected, quickly
135 frozen in liquid nitrogen. Three biological replicates were used for per cultivar. WJ1, WJ2 and
136 WJ3 represent samples from the WL712 cultivar. AJ1, AJ2 and AJ3 represent samples from the
137 Aohan cultivar. Finally, six samples were used for RNA-seq.

138 **Library construction and RNA-seq**

139 Total RNA was isolated from stems using the RNeasy Plant Mini Kit (Qiagen, Germany). A
140 total of 3 µg RNA per sample was used to build the library. Sequencing libraries were generated
141 using a NEBNext® Ultra™ RNA Library Prep Kit (NEB, USA). Messenger RNA was purified
142 from each sample using magnetic beads and fragmented with divalent cations at elevated 
143 temperature. First-strand cDNA was obtained using segmented mRNA as template and random
144 oligonucleotide as primer. Then, the second strand of cDNA was obtained in DNA polymerase I
145 system. The double-stranded cDNA were purified using AMPure XP Beads (Beckman Coulter,
146 Beverly, USA). The double-stranded cDNA was ligated to the sequencing adaptor after terminal
147 repair and A tail, and 250-300 bp cDNA was obtained using AMPure XP beads. Finally, the PCR
148 system was amplified, and the PCR products were purified again using AMPure XP beads to obtain
149 the libraries.

150 Library quality was examined using the Agilent Bioanalyzer 2100 system. The effective
151 concentration of the library (≥ 2 nM) was quantified using qRT-PCR. After passing the inspection,
152 the libraries were pooled and sequenced on the Illumina HiSeq X-10 (California, USA) platform
153 by Beijing Novo Biotech Company, Ltd. Finally, each sample contained an average of 6.63 G of
154 valid data, and 4.42×10^7 clean reads.

155 **Quality control**

156 To ensure the accuracy of data analysis, we filtered the original data and examined the
157 sequencing error rate. Using in-house Perl scripts to process the raw reads of fastq
158 format. Removing reads containing adapters, ploy-N sequences, and low-quality from the raw data
159 to obtain clean reads. The Q20, Q30, and GC contents of the clean data were calculated. All

160 subsequent analyses depend on clean data, high quality.

161 RNA-seq data analysis

162 The index of the reference genome was constructed using HISAT2 v2.2.1. The paired-end
163 clean reads were obtained using HISAT2 v2.2.1 (<https://cloud.biohpc.swmed.edu/index>) aligned to
164 the reference genome Zhongmu No. 1 ([https://figshare.com/articles/dataset/genome_fastq_sequence_and
165 annotation_files/12327602](https://figshare.com/articles/dataset/genome_fastq_sequence_and_annotation_files/12327602)) to obtain mapped reads (Mortazavi, Williams & McCue, 2008). We also
166 analysed of the proportion of mapped reads in the exons, introns, and intergenic regions of the
167 genome.

168 The clean reads aligned to Zhongmu No. 1 were quantified using FeatureCounts v1.5.0-p3.
169 Gene expression was tested by FPKM (fragments per kilobase of transcript per million fragments
170 mapped), and differences between WL712 and Aohan FPKM values were compared using
171 FeatureCounts v1.5.0-p3.

172 Differential expression analysis of the two comparison combinations was performed using
173 the DESeq2 R package (1.16.1) ([https://www.bioconductor.org/packages/release/bioc/html/DESeq
174 q2.html](https://www.bioconductor.org/packages/release/bioc/html/DESeq2.html)). DESeq2 determines the differential expression in digital gene expression data using a
175 model based on a negative binomial distribution. The corrected P-values and $|\log_2\text{foldchange}|$ are
176 thresholds for significant differential expression. P-values were adjusted using the Benjamini &
177 Hochberg method.

178 Gene Ontology (GO) (<http://www.geneontology.org/>) enrichment and KEGG (Kyoto
179 Encyclopedia of Genes and Genome) (<http://www.genome.jp/kegg/>) statistical analysis of DEGs
180 were performed using the clusterProfiler R package. A corrected P-value less than 0.05 was used
181 as the threshold for significant enrichment of differentially expressed genes.

182 qRT-PCR

183 The accuracy of the RNA-seq was verified by qRT-PCR. Total RNA were isolated from
184 stems, and cDNA was synthesised by using the PrimeScript™ RT reagent Kit (Takara, Tokyo,
185 Japan). Alfalfa *β-Actin 2* was used as the internal gene. The primers in **Table S9** were used for
186 qRT-PCR. qRT-PCR were completed using the LightCycler 96/LightCycler480 system. The
187 solution of the 20 μL system contained 0.4 μL forward primer, 0.4 μL Reverse Primer, 10 μL TB
188 Green Fast qPCR Mix (2X) (Takara, Tokyo, Japan) and 2 ng cDNA. The PCR procedure included
189 45 cycles, with 3 technical repeats for each reaction. According to Kenneth report, the relative
190 expression of each gene was calculated (Livak & Schmittgen, 2001).

191 Statistical Analysis

192 All statistical analysis was using SPSS software (version 17; IBM Inc, USA). The data were
193 compared using Student's t-test, and $P < 0.05$ was considered statistically significant. The power
194 of our samples was calculated using RNASeqPower ([https://bioconductor.org/
195 Packages/release/bioc/html/RNASeqPower.html](https://bioconductor.org/packages/release/bioc/html/RNASeqPower.html)), and the RNASeqpower was 94.2%.

196 Result

197 Phenotypic analysis of five alfalfa varieties

198 To compare the differences in the growth patterns of the five cultivars (**Table S1a**), plant
199 height, internode length and stem diameter of alfalfa at different growth stages were continuously
200 measured in 2019 and 2020 (**Fig. 1, Table S10**). There were no significant differences in plant

201 height, internode length or stem diameter among cultivars at the seedling transplant stage. After
202 the budding stage, plant height, internode length and stem diameter of different alfalfa varieties
203 reached a plateau and remained relatively stable (**Fig. 1a-c**). In 2019 and 2020, WL712 and Aohan
204 represented tall and short phenotypes, respectively, ~~in alfalfa~~ (**Fig. 1d**). Comparing the agronomic
205 traits of alfalfa at the budding stage in 2019 and 2020, the plant height of WL 712 was
206 approximately 1.78 and 1.91 times those of Aohan, respectively, and the stem diameter of WL 712
207 was approximately 1.90 and 1.92 times those of Aohan (**Fig. 1d-e**). The internode length and
208 number of lateral branches in WL712 were significantly larger than those in Aohan ($P < 0.01$),
209 whereas the number of main branches in WL712 was significantly lower ($P < 0.05$) (**Fig. 1f, Fig.**
210 **2a-b**).

211 To identify the correlation between internode length and stem diameter and other traits, the
212 fresh weight, leaf-stem ratio, and dry weight of the five cultivars were also determined. The results
213 showed that the production performances of WL712 and Aohan were significantly different ($P <$
214 0.05) (**Fig. 2c-f**). Phenotypic correlation analysis based on 8 agronomic traits was done. We found
215 that fresh and dry weight were positively and strongly correlated with the number of lateral
216 branches, plant height, stem diameter, and internode length, and plant height was significantly
217 positively correlated with internode length ($P < 0.01$). In addition, the number of main branches
218 was negatively correlated with plant height, stem diameter, and internode length ($P < 0.01$) (**Table**
219 **1**).

220 From the screening of five alfalfa cultivars, WL712 and Aohan were identified as the cultivars
221 with the most significant difference in growth performance. The growth trend of the two varieties
222 in greenhouse is similar to that in field. The plant height, internode length, yield per plant, leaf
223 area and stem diameter of WL712 alfalfa were significantly higher than those of Aohan alfalfa
224 (**Table 2**).

225 Based on the above results, WL712 and Aohan were used as ~~high-type~~ vigorous-growing and
226 ~~short-type~~ slow-growing experimental cultivars, while the stem base tissue was used for RNA-seq
227 (**Fig. S1**).

228 RNA-seq analysis

229 Using RNA-seq to obtain 2.74×10^8 raw reads. The sequence error rate of a single base
230 position was 0.03%, and the average GC content was 41.65%. After filtering from the raw data,
231 2.65×10^8 (96.94%) clean reads (39.76 G) were obtained. The Phred values were greater than 97%
232 and 93% at Q_{20} and Q_{30} , respectively (**Table S1c**). The Pearson coefficient showed that the
233 homology among the samples within the group was higher than 84.6% (**Fig. S2**).

234 We aligned the clean reads with the reference genome. The average proportions of exons,
235 introns and intergenic regions in AJ samples were 72.72%, 3.61%, and 23.67%, respectively.
236 Similarly, the WJ samples accounted for 74.14%, 2.96%, and 22.90%, respectively (**Table S2**).
237 The reads aligned to the intron region may have been derived from the precursor mRNA. The reads
238 aligned to the intergenic region may have been derived from ncRNAs.

239 Additionally, according to the comparison of RNA-seq data from WL 712 and Aohan, the
240 RNASeqpower of our sample was 94.2%. The result may be beneficial to screen and explore the
241 functional DEGs related to the vigorous-growing of alfalfa. These results demonstrated that the

242 experiments were reproducible and that the data were accurate.

243 **Identification and functional annotation of DEGs in WL712 and Aohan**

244 Generally, ~~FPKM is used to evaluate~~ the gene expression value of RNA-seq, which corrects
245 the sequencing depth and gene length successively (**Fig. S3**). More than 90% of the clean reads
246 were successfully mapped to the alfalfa genome. To clarify the function of the DEGs in WL712
247 and Aohan, we performed GO and KEGG enrichment analyses. In total, 954 remarkably enriched
248 DEGs were assigned to 35 GO terms. Compared to Aohan, WL712 upregulated 578 genes and
249 downregulated 376 genes. Among the molecular function, “*protein heterodimerization activity*”
250 [GO:0046982] (114 DEGs, 11.95%) was the highest proportion, followed by “*UDP-*
251 *glycosyltransferase activity*” [GO:0008194] (99 DEGs, 1.04%) and “*translation factor activity,*
252 *RNA binding*” [GO:0008135] (86 DEGs, 9.01%). Among the cell components, “*-bounding*
253 *membrane of organelle-*” [Go:0098588] (57 DEGs, 5.97%) represented the largest cluster,
254 followed by “*whole membrane*” [Go:0098805] (49 DEGs, 5.13%) and “*peptidase complex*”
255 [Go:1905368] (44 DEGs, 4.61%). Among the biological processes, “*translational elongation*”
256 [GO:0006414] (41 DEGs, 4.30%) represented the largest cluster (**Table 3, Table S3 , Fig. 3a**).

257 Based on biological system network, the function of DEG was identified using KEGG
258 classification. A total of 1324 genes were enriched in 110 KEGG pathways (**Fig. 3b**). “*Carbon*
259 *metabolism*” [ath01200] (103 DEGs, 7.8%) and “*Ribosome*” [ath03010] (96 DEGs, 7.3%) were
260 the most abundant pathways; followed by “*Biosynthesis of amino acids*” [ath01230] (81 DEGs,
261 6.1%), “*RNA transport*” [ath03013] (54 DEGs, 4.1%), “*Plant-pathogen interaction*” [ath04626]
262 (52 DEGs, 3.9%), “*Protein processing in endoplasmic reticulum*” [ath04141] (52 DEGs, 3.9%)
263 and “*Plant hormone signal transduction*” [ath04075] (44 DEGs, 3.2%) (**Table S4**).

264 **Expression and regulation of DEGs in WL712 and Aohan**

265 KEGG analysis showed that DEGs related to stem elongation and diameter enlargement were
266 widely involved in biological processes such as hormone signalling, photosynthesis and
267 transcriptional regulation (**Table S5**).

268 Plant hormone signal ~~transformation~~ (Ath04075) involves many hormones that regulate the
269 growth and development ~~of plants~~, such as auxins, cytokinines, gibberellins, brassinosteroids,
270 jasmonic acid, and ethylene. Twelve DEGs were enriched in the auxin-mediated signalling
271 pathway, including *auxin-responsive protein SAUR (SAUR)*, *auxin-induced protein X10A* (new
272 gene) and *auxin transporter-like protein (LAX)*. Among these, *IAA9*, *IAA6*, *SAUR50*, *SAUR32* and
273 *SAUR36* were significantly upregulated. In the cytokinin-mediated signalling pathway, four DEGs
274 were enzyme genes, such as *adenylate isopentenyltransferase 5 (IPT5)*, *7-deoxyloganetin*
275 *glucosyltransferase (UGT85A24)*, *cytokinin dehydrogenase 6 (CKX6)*, and *cytokinin hydroxylase*
276 *(CYP735A2)*. *DELLA protein GAI (GAI)*, *f-box protein GID2 (GID2)*, and *transcription factor*
277 *PIF4 (PIF4)* were enriched in the gibberellin-mediated signalling pathway. *Serine/threonine-*
278 *protein kinase BSK8 (BSK8)*, *serine/threonine-protein kinase BSK1 (BSK1)*, and *Cyclin-D3-3*
279 *(CYCD3-3)* were enriched in the brassinosteroid-mediated signalling pathway. Five DEGs were
280 enriched in the jasmonic mediated signalling pathway, including *Coronatine-insensitive protein*
281 *homolog 1a (COII A)*, *Protein TIFY 6 B (TIFY 6B)*, *Protein TIFY 11 B (TIFY 6B)*, *Protein TIFY*
282 *10 B (TIFY 10B)* and *Protein TIFY 3 B (TIFY 3B)*. Four upregulated DEGs were enriched in the

283 ethylene-mediated signalling pathway, including *ethylene receptor (ETR 1)*, *mitogen-activated*
284 *protein kinase kinase 4 (MKK 4)*, *mitogen-activated protein kinase homolog MMK1 (MMK 1)*, and
285 *protein ethylene insensitive 3 (EIN 3)*.

286 Fifteen DEGs were enriched in the photosynthetic (ath00195) pathway. Among them, *PPLI*,
287 *PETC*, *PSBR*, *PSBS*, *PSAG*, *PSAO*, *PSB 27* and *PSB 28* were related to the photoreaction. *PLSN*
288 *2* was related to the activity of the chloroplast NAD(P)H dehydrogenase (NDH) complex. *ATPF*
289 *2* and *ATPC* are related to ATPase activity. Additionally, two oxygen-evolving enhancer proteins
290 and ferredoxins have been identified. In the photosynthesis-antenna protein (ath00196) pathway,
291 eleven DEGs were classified into *chlorophyll a-b binding proteins* and *chlorophyll a/b binding*
292 *proteins*, which were expressed in chloroplasts. In the MAPK signalling (ath04016) pathway,
293 twenty-two DEGs were mainly involved in biotic stress (pathogen infection), abiotic stress
294 (cold/salt/drought/osmotic stress), and hormone synthesis during root growth and wounding
295 responses.

296 Furthermore, the TCA cycle (ath00020), carbon fixation in photosynthetic organisms
297 (ath00710), glycolysis/gluconeogenesis (ath00010), ribosome (ath03010), amino sugar and
298 nucleotide sugar metabolism (ath00520), pyruvate metabolism (ath00620), and phenylpropanoid
299 biosynthesis (ath00940) were also closely related to alfalfa growth (**Table S5**). In the TCA cycle
300 pathway, 12 DEGs played a role in catalysis of the pyruvate dehydrogenase complex. In addition,
301 *ATP-citrate synthase alpha chain protein 1 (ACLA 1)* and *2 malate dehydrogenases (MDH)* were
302 identified. *Pyrophosphate--fructose 6-phosphate 1-phosphotransferase subunit beta (PFM)* and
303 *glycoaldehyde-3-phosphate dehydrogenase (GAPC1)* were highly expressed in the
304 glycolysis/gluconeogenesis pathway. Seven *glyceraldehyde-3-phosphate dehydrogenases*
305 (*GAPDH*) were enriched in carbon fixation in the photosynthetic organism pathway and were
306 highly expressed in the cytoplasm or chloroplasts. Ribosomal proteins predominated in the
307 ribosomal pathway and included 30 s (*RPS 1*, *RPS 13*, *RPSQ*, *RPS 16*), 40 s (*RP 24 a*, *RP 30 a*,
308 *RP 15 d*, *RP 10 a*, *RP 20 a*), 50 s (*RPL 28*, *RPMJ*, *RPL 31*, *RPLX*) and 60 s (*RPP 3 a*, *RPL 21 e*,
309 *RPL 37a*, *RPL 37 B*). *Dihydrolipoyllysine-residue acetyltransferase component 2 of the pyruvate*
310 *dehydrogenase complex (At3g13930)* and *malate dehydrogenase (mMDH)* were highly expressed
311 in the pyruvate metabolic pathway. *Beta-glucosidase 44 (BGLU 44)*, *beta-amylase 1 (BAM 1)*,
312 *acid beta-fructofuranosidase (VCINV)*, and *probable fructokinase-4 (At3g59480)* were highly
313 expressed in the starch and sucrose metabolism pathways. The genes with high expression in the
314 phenylpropanoid biosynthesis pathway were *Probable cinnamyl alcohol dehydrogenase (CAD 2)*,
315 *beta-glucosidase 46 (BGLU 46)*, *trans-cinnamate 4-monooxygenase (CYP 73A3)*, and *3*
316 *peroxidases (PER)*.

317 **DEGs enriched in a variety of biological processes**

318 All DEGs were analysed using GO and KEGG analyses. We found that seven groups of DEGs
319 related to stem elongation and diameter expansion, including formation of water-conducting tissue
320 in vascular plants, cell division and shoot initiation, biosynthesis and degradation of lignin, cell
321 enlargement and plant growth, formation of the primary or secondary cell wall, cell elongation,
322 and stem growth and induced germination (**Table S6**). *Eukaryotic translation initiation factor 5A-*
323 *1 (EIF 5A)*, *mitogen-activated protein kinase kinase kinase 3 (ANP 3)*, and *alpha, alpha-trehalose-*

324 *phosphate synthase (TPS 6)* were involved in the formation of water-conducting tissues. Fourteen
325 DEGs were enriched in lignin biosynthesis and degradation. Peroxidases play an important role in
326 this process. Additionally, *peroxidase 47 (PER 47)* is a novel gene. Eleven DEGs were enriched
327 in the formation of the primary or secondary cell wall. *Cellulose synthase A catalytic subunit*
328 (*CESA*) plays an active role. Eighteen DEGs were enriched in cell enlargement and plant growth.
329 AUXs, such as *auxin-responsive protein (IAA 9)*, *auxin-induced protein (IAA 6)* and *auxin*
330 *transporter-like protein (LAX 5)*, play an active role. Additionally, *auxin-induced protein XI0A* is
331 a novel gene. Five DEGs were enriched in cell division and shoot initiation. Enzyme genes such
332 as *7-deoxyloganetin glucosyltransferase (UGT 85A24)*, *cytokinin hydroxylase (CYP 735A2)* and
333 *cytokinin dehydrogenase 6 (CKX 6)* play a dominant role. Two DEGs were enriched in stem
334 growth and induced germination. Interestingly, *DELLA protein (GAI)* negatively regulated the
335 gibberellin signalling pathway, whereas *F-Box protein (GID 2)* positively regulated the gibberellin
336 signalling pathway. *Serine/threonine-protein kinase (BSK 1)* and *BSK 8* are related to cell
337 elongation. Additionally, we identified genes that regulate senescence, including *protein ethylene*
338 *insensitive 3 (EIN 3)*. Importantly, compared with Aohan, *cellulose synthase A catalytic subunit 8*
339 (*CESA 8*), *beta-1,4-xylosyltransferase (IRX 9)*, *probable beta-1,4-xylosyltransferase (IRX 14H)*,
340 *auxin-responsive protein (SAUR 36)*, *peroxidase 16 (PER 16)*, and *peroxidase 51 (PER 51)* were
341 upregulated more than 8-fold in WL712, whereas *mitogen-activated protein kinase 3 (MPK 3)*,
342 *pathogenesis-related protein (At2g14610)*, *peroxidase 55 (POD 55)*, *beta-glucosidase 46 (BGLU*
343 *46)*, and *peroxidase 15 (POD 15)* were downregulated more than 15-fold in WL712 (**Table S7**).
344 All the genes related to stem growth and development were clustered together, as shown in **Fig. 4**.

345 **TFs involved in alfalfa growth and development**

346 **TFs** are essential in plant growth and development as protein molecules that regulate gene
347 expression. In this study, 20 TFs were involved in the development of alfalfa (**Fig. 5a, Table S8**).
348 Seven DEGs were upregulated, including *NAC domain-containing protein 73 (NAC073)*, *NAC*
349 *domain-containing protein 10 (NAC010)*, *transcription factor MYB 46 (MYB 46)*, and *NAP-related*
350 *protein 2 (NRP2)*. Additionally, *WRKY transcription factor 22 (WRKY 22)*, *transcription factor*
351 *TGAI (TGAI)* and *Transcription factor MYB 86 (MYB 86)* were novel genes. GO annotations
352 revealed that *NAC073* and *NAC010* were involved in the synthesis of cellulose and hemicellulose
353 and the development of secondary cell wall fibres. Thirteen DEGs were downregulated, and the
354 *WRKY* and *MYB* family members played a dominant role. GO classification shows that *WRKY 51*
355 was involved in the positive regulation of salicylic acid-mediated signal transduction and negative
356 regulation of jasmonic acid-mediated signal transduction in the defense respons. *WRKY 54* is a
357 negative regulator of plant growth and development. *MYB 46* is involved in secondary wall
358 cellulose biosynthesis as a transcriptional activator. *MYB 86* is involved in lignin synthesis and
359 accumulation. Additionally, *MYB 2* inhibited the expression of light-harvesting genes. All
360 identified TFs were validated using qRT-PCR (**Fig. 5b**). The relative expression of *NAC 081* was
361 significantly upregulated in WL 712 plant ($P < 0.001$). The relative expression levels of most TFs
362 were similar to the the FPKM trend.

363 **The reliability of RNA-seq was verified using qRT-PCR**

364 To determine the accuracy and rationality of the data, we randomly selected 11 DEGs for

365 qRT-PCR validation. DEGs were mainly related to the formation of the primary or secondary cell
366 wall, cell enlargement and plant growth, and biosynthesis and degradation of lignin. The changes
367 in transcript abundance are shown in **Fig. 6a**. qRT-PCR revealed that *IRX 9*, *CESA 8*, *CESA 7*,
368 *MKK 4*, *PER 16*, and *PER 51* were significantly upregulated in WL712 plant ($P < 0.05$). *MPK 3*,
369 *At2g14610*, *BGLU 46*, and *POD 15* were significantly downregulated in WL 712 ($P < 0.05$) (**Fig.**
370 **6b**). However, the relative expression of *CAD 2* between the two varieties were not significantly
371 different ($P > 0.05$) and were inconsistent according to RNA-seq transcript abundance. This may
372 have been caused by RNA-seq errors in the acceptable range. Overall, the relative expression trend
373 of the DEGs was similar to the RNA-seq.

374 Discussion

375 Alfalfa is an important component of feed, and the growth performance of its aboveground
376 part affect the grass yield. The *FmS6K* plays an important role in regulating the development of
377 plant stems (Sun et al., 2018). The yield of elephant grass has a strong positive correlation with
378 internode length (Yan et al., 2021). However, the molecular regulatory mechanisms underlying
379 the vigorous-growing of stems and branches in alfalfa remain unclear. In this study, the growth
380 difference between vigorous and fast-growing variety WL712 and short and slow-growing variety
381 Aohan alfalfa varieties was studied by comprehensive method. The phenotypes and RNA-seq of
382 these two varieties were analyzed by using stems. The results of qRT-PCR showed that the
383 expression trend of most DEGs was consistent with RNA-seq. The difference between qRT-PCR
384 and RNA-seq of individual DEG may be caused by the error of RNA-seq within the acceptable
385 range. Overall, the RNA-seq data could be used for subsequent analysis. All DEGs were enriched
386 with GO; 954 significant DEGs were obtained, and seven DEG clusters were involved in
387 regulating the vigorous-growing of alfalfa (**Fig. 4**). Additionally, KEGG revealed that hormone
388 signal transduction, photosynthesis and phenylpropane biosynthesis regulate the process of the
389 vigorous-growing of alfalfa. RNA-seq also identified several novel DEGs associated with the
390 vigorous-growing of alfalfa, including *PER47* and *TIFY10A*.

391 Plant organ growth is regulated by both developmental processes and environmental factors
392 (Sun et al., 2018). In most cases, these changes are mainly due to hormone-mediated action
393 (Verma, Ravindran & Kumar, 2016). In this study, auxin, cytokinin, gibberellin, ethylene,
394 brassinosteroid, and jasmonic acid affected the growth and development of alfalfa by regulating
395 downstream DEGs, such as *SAUR50*, *CKX6*, *GID2*, and *GAI*. These DEGs might play a role in the
396 vigorous-growing of alfalfa. Previous studies have identified *SAURs* as a class of hormones that
397 regulate plant growth and development and promote cell enlargement (Ren & Gray, 2015).
398 Cytokinin biosynthesis was required to activate shoot division in apple trees with the top removed
399 (Tan et al., 2018). Relevant studies have shown that gibberellin regulates plant organ elongation
400 and development (Nagel, 2020). *GAI* is an inhibitor of highly conserved gibberellin (*GA*)
401 signalling in plants. The *SCF (GID2)* complex mediates degradation of DELLA proteins (*RLG2*,
402 *RGA*, and *GAI*), and activates and positively regulates the gibberellin signalling pathway (Dill et
403 al., 2004). In addition, in the plant hormone signal transduction pathway, the production of
404 hormones that play a mediating role depends on the metabolism of amino acids or fatty acids.
405 Tryptophan in plants is not only involved in the synthesis of its own proteins but also the precursor

406 of many ~~secondary~~ metabolites (such as auxin) (Manol & Nemoto, 2012). Jasmonic acid induces
407 plants to prioritise defense over growth by interfering with the gibberellin signalling cascade,
408 which is usually accompanied by significant growth inhibition (Yang et al., 2012). *TIFY*, which
409 encodes jasmonic acid repressor, was significantly upregulated in Aohan (**Table S5**). This may
410 explain why the **low-dormancy** alfalfa plant is a dwarf.

411 Photosynthesis is an essential metabolic process ~~that regulates the growth and yield of plant~~.
412 Twenty-nine DEGs were related to photosynthesis. For example, *PIF1* and *PIF3* were significantly
413 downregulated in WL712 (**Table S5**). These genes may play a regulatory role in the process of
414 plant height and internode elongation. Plant height, and leaf area of transgenic soybean ~~were~~
415 decreased by overexpressing *PIF4* (Arya, Singh & Bhalla, 2021). The deletion of *PIF1* and *PIF3*
416 results in an increase in plant height, longer internodes, and late flowering (Hoang et al., 2021).
417 The light-harvesting complex II (LHC II) functions as a light receptor and is related to the
418 absorption of light (Gu et al., 2017; Sen et al., 2021). The up-regulation of these DEGs may
419 enhance the photosynthesis of WL712 and promote the growth of plants. Additionally, circadian
420 rhythm is also involved in the regulation of plant growth and development (Venkat & Muneer,
421 2022). Our research found that DEGs enriched in circadian rhythm pathway were mainly related
422 to photoperiod flowering response. (**Table S5**).

423 Driven by differences in plant tissue growth, cells continue to divide, proliferate and
424 differentiate, eventually forming various functional organs (Huang et al., 2018; Hilde &
425 Nathalie, 2020). RNA-seq analysis showed that 1531 DEGs related to rape stem growth (Yuan
426 et al., 2019). Combined analysis of proteome and RNA-seq showed that DEGs and DEPs of
427 **Mikania micrantha** stems were significantly enriched in photosynthesis, carbon sequestration and
428 plant hormone signal transduction pathways (Can et al., 2021). We identified seven DEG clusters
429 that were involved in stem elongation and enlargement. Fourteen DEGs were enriched in lignin
430 biosynthesis and degradation (**Fig. 4a**) ~~and mainly consisted of~~ peroxidase. Eleven DEGs were
431 involved in the formation of the primary or secondary cell wall (**Fig. 4b**), ~~and mainly consisted of~~
432 cellulose synthase. ~~These genes may regulate lignin biosynthesis and degradation in stems.~~
433 Previous studies reported that *CESA4* and *CESA8* were specifically enriched and expressed in the
434 stem tissue during the fibre development stage (Guo et al., 2021). ~~The oxidation activity of~~
435 ~~peroxidases is limited to the lignified region during plant development (Hoffmann et al., 2020).~~
436 Eighteen DEGs were enriched in cell enlargement and plant growth (**Fig. 4c**) ~~and mainly consisted~~
437 ~~of~~ auxin. Five DEGs were involved in cell division and shoot initiation (**Fig. 4e**). ~~Interestingly,~~
438 ~~*TPS6* was also involved in the formation of water-conducting tissues (Fig. 4h).~~ Two DEGs were
439 enriched in the processes of stem growth and induced germination (**Fig. 4f**), ~~which mainly affected~~
440 ~~plant growth and development by regulating the gibberellin signalling pathway.~~ Two DEGs were
441 ~~found to be~~ involved in cell elongation (**Fig. 4g**). These DEGs might play a role in stem internode
442 elongation, diameter enlargement and lateral branch formation. ~~Previous studies reported that~~
443 ~~*AtTPS6* completely compensates for the defects in reduced trichome and stem branching due to~~
444 ~~*esp-1* deficiency in Arabidopsis (Chary et al., 2008).~~ Deletion of *IAA17* in tomatos showed that
445 the increase in fruit size was related to the higher ploidy level of peel cells (Su et al., 2015). Finally,
446 the *TIFY* homologous related to alfalfa senescence were also identified (**Fig. 4d**). In addition, we

447 identified several members of *SPL* family, such as *SPL1*, *SPL6* and *SPL7*, which may be involved
448 in the lateral branch development of alfalfa. Previous studies reported that *SPL13* regulates shoot
449 branching in *Medicago sativa* (Gao et al., 2018). Overall, these DEGs may be involved in alfalfa
450 growth and development.

451 **TFs** are essential in the regulation of development, morphogenesis and environmental stress
452 ~~in higher plants. Our~~ research found that most members of *NAC*, *WRKY* and *MYB* families were
453 involved in the biosynthesis of lignin, cellulose and hemicellulose (Wang et al., 2016). The *NAC*-
454 mediated transcription network synergistically regulated biosynthesis of the plant secondary wall
455 (Ryan, Zhong & Ye, 2011). *WRKY6* and *WRKY33* positively regulated ABA signal transduction
456 during early development of *Arabidopsis thaliana* (Huang et al., 2016). *WRKY54* is a negative
457 regulator of salicylic acid (*SA*) biosynthesis (Li, Zhong & Palva, 2017) and can significantly
458 increase stem diameter, leaf area, and total dry weight of plants (Amin et al., 2013).
459 Overexpression of *AtMYB44* in tomatoes resulted in slow growth (Shim et al., 2012). *MYB3R1* is
460 a transcriptional repressor that regulates organ growth, and restricts plant growth and development
461 by binding to target genes and promoters of specific genes (Wang et al., 2018). Under reduced
462 light intensity, *MYB2* and *MYR1* acted as inhibitors of flowering and organ elongation, respectively
463 (Zhao et al., 2011). In this study, excluding for *WRKY 22*, all *WRKY* members were significantly
464 upregulated in dwarf alfalfa. Therefore, *WRKY 22* may positively regulate the growth and
465 development of WL712. *NACs* are involved in the development of plant secondary cell walls.
466 Among these, *NAC081* functions as a positive regulator. *MYB46* and *MYB86* positively regulate
467 the synthesis of plant cellulose and lignin, and *MYB44*, *MYB3R1* and *MYB2* act as transcriptional
468 repressors (**Table S8**).

469 **Conclusion**

470 Plant height is a important factor in determining forage biomass. The molecular
471 characteristics of the DEGs ~~that regulate the vigorous-growing of alfalfa in WL 712 and Aohan~~
472 ~~alfalfa~~ were identified using RNA-seq. The trend of our qRT-PCR was largely consistent with
473 those of RNA-seq, which indicated that the RNA-seq data could be used for subsequent analysis.
474 All DEGs were analysed using GO enrichment, and 954 significant DEGs were identified. KEGG
475 analysis indicated that hormone signal transduction, phenylpropane biosynthesis, and
476 photosynthesis ~~are involved in the regulation of the vigorous-growing of alfalfa~~. GO analysis
477 ~~revealed that~~ seven clusters of DEGs ~~engaged in the~~ formation of water-conducting tissue ~~in~~
478 ~~vascular plants~~, cell division and shoot initiation, biosynthesis and degradation of lignin, stem
479 growth, formation of the primary or secondary cell wall, cell enlargement and plant growth, and
480 induced germination and cell elongation. Additionally, the **TFs involved** in stem elongation and
481 diameter expansion are mainly *WRKY*, *NAC*, and *MYB* family members. In summary, our research
482 results not only enrich the transcriptome database of alfalfa, but also provide valuable information
483 for explaining the molecular mechanism of ~~fast-growing~~, and can provide reference for the actual
484 production of alfalfa at the same latitude and similar soil in the world.

485 **Competing Interests**

486 The authors declare there are no competing interests.

487 **Author Contributions**

488 Qi Jiangjiao conceived and designed the experiments, performed the experiments, analyzed
489 the data, prepared Fig.s and/or tables, and authored or reviewed drafts of the paper.

490 Yuxue, Wang Xuzhe and Zhang Fanfan performed the experiments.

491 Ma Chunhui conceived and designed the experiments, performed the experiments, analyzed
492 the data, authored or reviewed drafts of the paper, and approved the final draft.

493 **Availability of data and materials**

494 The data is available at the Sequence Read Archive (SRA) of NCBI:
495 <https://www.ncbi.nlm.nih.gov/sra/?term=PRJNA807394>.

496 **Funding**

497 This work was supported by China Agriculture Research System of MOF and MARA.

498 **Reference**

499 Aung B, Gruber M, Amyot L, Omari K, Bertrand A, Hannoufa A. 2015. Ectopic expression of
500 LjmiR156 delays flowering, enhances shoot branching, and improves forage quality in alfalfa.

501 *Plant Biotechnology Reports* 9(6):379-393

502 Arshad M, Gruber MY, Hannoufa A. 2018. Transcriptome analysis of microRNA156
503 overexpression alfalfa roots under drought stress. *Scientific Reports* 8:9363

504 Arya H, Singh MB, Bhalla PL. 2021. Overexpression of PIF4 affects plant morphology and
505 accelerates reproductive phase transitions in soybean. *Food and Energy Security* 10(3):1

506 **Amin AA**, El-Kader AA Abd, Shalaby MAF, Gharib FAE, Rashad ESM, Teixeira da SJA. 2013.
507 Physiological Effects of Salicylic Acid and Thiourea on Growth and Productivity of Maize
508 Plants in Sandy Soil. *Communications in Soil Science & Plant Analysis* 44(7):1141-1155

509 Bambang S, Lukmana A, Nafiatul U, Bambang S. 2021. The performance and genetic variation of
510 first and second generation tropical alfalfa (*Medicago sativa*). *Biodiversitas* 22(6)

511 Celebi SZ, Kaya L, Sahar AK, Yergin R. 2010. Effects of the **Weed Density** on Grass Yield of
512 Alfalfa. In Different Row Spacing Applications. *African Journal of Biotechnology* 9(41):6867-
513 6872

514 Chen L, Yang Y, K Mishina, Cui C, Zhao Z, Duan S, Chai Y, Su R, Chen F, Hu Y.G. 2020. RNA-
515 seq analysis of the peduncle development of Rht12 dwarf plants and primary mapping of Rht12
516 in common wheat. *Cereal Research Communications* 48(2):139-14

517 Cui C, Wang Z, Su YJ, Wang T. 2021. New insight into the rapid growth of the *Mikania micrantha*
518 stem based on DIA proteomic and RNA-seq analysis. *Journal of proteomics*: 104126

519 Chary SN, Hicks GR, Choi YG, Carter D, Raikhel NV. 2008. Trehalose-6-phosphate
520 synthase/phosphatase regulates cell shape and plant architecture in *Arabidopsis*. *Plant*
521 *physiology* 146(1):97-107

522 Diatta AA, Doohong M, Jagadish SVK. 2021. Chapter Two - Drought stress responses in non-
523 transgenic and transgenic alfalfa--Current status and future research directions. *Advances in*
524 *Agronomy*:35-100

525 Dill A, Thomas SG, Hu JH, Steber CM, Sun TP. 2004. The *Arabidopsis* F-box protein SLEEPY1
526 targets gibberellin signaling repressors for gibberellin-induced degradation. *Plant Cell*
527 16(6):1392-1405

528 Ernest BA, Alena PB, Mariam RS, Marian O, Edo G, Henk VA, Richard GFV, C Gerard VDL.

- 529 2020. Morphological and physiological responses of the potato stem transport tissues to
530 dehydration stress. *Planta* 251(2):45
- 531 Etzold S, Sterck F, Bose AK, Braun S, Buchmann N, Eugster W, Gessler A, Kahmen A, Peters
532 RL, Vitasse Y, Walthert L, Ziemińska Kasia, Zweifel R, Penuelas J. 2021. Number of growth
533 days and not length of the growth period determines radial stem growth of temperate trees.
534 *Ecology letters* 25:427– 43
- 535 Fan WQ, Ge GT, Liu YH, Wang W, Liu LY, Jia YS. 2018. Proteomics integrated with
536 metabolomics: analysis of the internal causes of nutrient changes in alfalfa at different growth
537 stages. *BMC Plant Biology* 18 (1):78
- 538 Gao RM, Austin RS, Amyot L, Hannoufa A. 2016. Comparative transcriptome investigation of
539 global gene expression changes caused by miR156 overexpression in *Medicago sativa*. *BMC*
540 *genomics* 17(1):658
- 541 Guo JD, Huang Z, Sun JL, Cui XM, Liu Y. 2021. Research Progress and Future Development
542 Trends in Medicinal Plant Transcriptomics. *Frontiers in plant science*:691838
- 543 Gu JF, Zhou ZX, Li ZK, Chen Y, Wang ZQ, Zhang H, Yang JC. 2017. Photosynthetic Properties
544 and Potentials for Improvement of Photosynthesis in Pale Green Leaf Rice under High Light
545 Conditions. *Frontiers in plant science*:1082
- 546 Guo Y, Wen L, Chen JK, Pan G, Wu ZM, Li Z, Xiao QM, Wang YC, Qiu CS, Long SH, Zhao
547 XL, Wang H, Wang YF. 2021. Comparative Transcriptomic Analysis Identifies Key Cellulose
548 Synthase Genes (CESA) and Cellulose Synthase-like Genes (CSL) in Fast Growth Period of
549 Flax Stem (*Linum Usitatissimum* L). *Journal of Natural Fibers*:1-16
- 550 Hoang QTN, Tripathi S, Cho JY, Choi DM, Shin AY, Kwon SY, Han YJ, Kim JI. 2021.
551 Suppression of Phytochrome-Interacting Factors Enhances Photoresponses of Seedlings and
552 Delays Flowering With Increased Plant Height in *Brachypodium distachyon*. *Frontiers in plant*
553 *science*:756795
- 554 Huang CJ, Wang ZL, David Quinn, Subra Suresh, K Jimmy Hsia. 2018. Differential growth and
555 shape formation in plant organs. *Proceedings of the National Academy of Sciences of the*
556 *United States of America* 115 (49):12359-12364
- 557 Hilde N, Nathalie G. 2020. Understanding plant organ growth: a multidisciplinary field. *Journal*
558 *of Experimental Botany* 71(1):7-10
- 559 Hoffmann N, Benske A, Betz H, Schuetz M, Samuels AL. 2020. Laccases and peroxidases co-
560 localize in lignified secondary cell walls throughout stem development. *Plant physiology*
561 184(2):806-822
- 562 Huang Y, Feng CZ, Ye Q, Wu WH, Chen YF. 2016. Arabidopsis WRKY6 Transcription Factor
563 Acts as a Positive Regulator of Abscisic Acid Signaling during Seed Germination and Early
564 Seedling Development. *PLOS Genetics* 12(2):e1005833
- 565 Jaykumar JC, Mahendra LA. 2016. In Vitro Callus Induction and Plant Regeneration from Stem
566 Explants of *Ceropegia noorjahaniae*, a Critically Endangered Medicinal Herb. *Methods in*
567 *molecular biology*:347-355
- 568 Kleyer M, Trinogga J, Cebrin-Piqueras MA, Trenkamp A, Fljgaard C, Ejrns R, Bouma TJ, Minden
569 V, Maier M, Mantilla CJ, Albach DC, Blasius B, Barua D. 2019. Trait correlation network



- 570 analysis identifies biomass allocation traits and stem specific length as hub traits in herbaceous
571 perennial plants. *Journal of Ecology* 107(2):829-842
- 572 Kumar T, Bao AK, Bao Z, Wang F, Gao L, Wang SM. 2018. The progress of genetic improvement
573 in alfalfa (*Medicago sativa* L). *Czech Journal of Genetics and Plant Breeding* 54(2):41-51
- 574 Kim S, Cho K, Lim SH, Goo TW, Lee JY. 2021. Transcriptome profiling of transgenic rice seeds
575 lacking seed storage proteins (globulin, prolamin, and glutelin) by RNA-seq analysis. *Plant*
576 *Biotechnology Reports* (1):77-93
- 577 Katyayini NU, Rinne PLH, Tarkowska D, Strnad M, Schoot C. 2020. Dual Role of Gibberellin in
578 Perennial Shoot Branching: Inhibition and Activation. *Frontiers in plant science*:736
- 579 Livak KJ, Schmittgen TD. 2001. Analysis of relative gene expression data using real-time
580 quantitative PCR and the $2^{-\Delta\Delta CT}$ method. *Methods* 25(4): 402-408
- 581 Li J, Zhong R, Palva ET. 2017. WRKY70 and its homolog WRKY54 negatively modulate the cell
582 wall-associated defenses to necrotrophic pathogens in Arabidopsis. *Plos One* 12(8):1-22
- 583 Martin N, Brink G, Shewmaker G, Undersander D, Walgenbach R, Hall M. 2010. Changes in
584 Alfalfa Yield and Nutritive Value within Individual Harvest Periods. *Agronomy Journal*
585 102(4):1274-1282
- 586 Monirifar H. 2011. Path Analysis of Yield and Quality Traits in Alfalfa. *Notulae Botanicae Horti*
587 *Agrobotanici Cluj-Napoca* 39(2):190-195
- 588 Mortazavi A, Williams BA, McCue K. 2008. Mapping and quantifying mammalian transcriptomes
589 by RNA-seq. *Nature methods* 5(7):621-628
- 590 Manol Y, Nemoto K. 2012. The pathway of auxin biosynthesis in plant. *J Exp Bot* 63:2853-2872
- 591 Nagel R. 2020. Gibberellin Signaling in Plants: Entry of a new MicroRNA Player. *Plant*
592 *physiology* 183(1):5-6
- 593 Ren H, Gray WM. 2015. SAUR Proteins as Effectors of Hormonal and Environmental Signals in
594 Plant Growth. *Molecular Plant* 8(8):1153-1164
- 595 Ryan LM, Zhong RQ, Ye ZH. 2011. Secondary wall NAC binding element (SNBE), a key cis-
596 acting element required for target gene activation by secondary wall NAC master switches.
597 *Plant signaling & behavior* 6(9):1282-1285
- 598 Sulc RM, Arnold AM, Cassida KA, Albrecht KA, Hall MH, Min D, Xu X, Undersander DJ, Santen
599 E. 2021. Changes in forage nutritive value of reduced-lignin alfalfa during regrowth. *Crop*
600 *Science* 61(2):1478-1487
- 601 Sena G. Stem cells and regeneration in plants(Article). 2014. *Nephron – Experimental Nephrology*
602 126 (2):5-39
- 603 Sun H, Zhao XT, Liu Z, Yang K, Wang Y, Zhan YG. 2018. Bioinformatics of S6K Genes in
604 *Fraxinus mandshurica* and Their Expression Analysis under Stress and Hormone. *Plant*
605 *research* 38(5):714-724
- 606 Sen S, Mascoli V, Liguori N, Croce R, Visscher L. 2021. Understanding the Relation between
607 Structural and Spectral Properties of Light-Harvesting Complex II. *The journal of physical*
608 *chemistry. A* 125(0): 4313-4322
- 609 Su LY, Audran C, Bouzayen M, Roustan JP, Chervin C. 2015. The Aux/IAA, SI-IAA17 regulates
610 quality parameters over tomato fruit development. *Plant Signaling & Behavior*

- 611 10(11):e1071001
- 612 Shim JS, Jung C, Lee S, Min K, Lee YW, Choi Y, Lee JS, Song JT, Kim JK, Choi YD. 2012.
- 613 AtMYB44 regulates WRKY70 expression and modulates antagonistic interaction between
- 614 salicylic acid and jasmonic acid signaling. *The Plant Journal* 73 (3):483-495
- 615 Tetteh JP, Bonsu KO. 1997. Agronomic performance of seven cultivars of alfalfa (*Medicago sativa*
- 616 L.) in the coastal savanna zone of Ghana. *Ghana Journal of Agricultural Science* 30(1):39-44
- 617 Tan M, Li GF, Qi SY, Liu XJ, Chen XL, Ma JJ, Zhang D, Han MY. 2018. Identification and
- 618 expression analysis of the IPT and CKX gene families during axillary bud outgrowth in apple
- 619 (*Malus domestica* Borkh). *Gene*:106-117
- 620 Verma V, Ravindran P, Kumar PP. 2016. Plant hormone-mediated regulation of stress responses.
- 621 *BMC Plant Biology* 16:1–10
- 622 Venkat Ajila, Muneer Sowbiya. 2022. Role of Circadian Rhythms in Major Plant Metabolic and
- 623 Signaling Pathways. *Frontiers in plant science* 13: 836244 DOI 10.3389/fpls.2022.836244
- 624 Wang J, Tang F, Gao CP, Gao X, Xu B, Shi FL. 2021. Comparative transcriptome between male
- 625 fertile and male sterile alfalfa (*Medicago varia*). *Physiology and Molecular Biology of Plants*
- 626 27(7):1487-1498
- 627 Wang Z, Gerstein M, Snyder M. 2009. RNA-seq: a revolutionary tool for transcriptomics. *Nature*
- 628 *Reviews Genetics* 10(1):57-63
- 629 Wang YJ, Li MC, Wu Wang, Wu HY, Xu YN. 2013. Cloning and Characterization of an
- 630 AP2/EREBP Gene TmAP2-1 from *Tetraena mongolica*. *Bulletin of Botany* 48(1):23-33
- 631 Wang HZ, Yang JH, Chen F, Ivone Torres-Jerez, Tang YH, Wang MY, Du Q, Cheng XF, Wen
- 632 JQ, Richard Dixon. 2016. Transcriptome analysis of secondary cell wall development in
- 633 *Medicago truncatula*. *BMC genomics*:23
- 634 Wang WP, Sijacic P, Xu PB, Lian HL, Liu ZC. 2018. Arabidopsis TSO1 and MYB3R1 form a
- 635 regulatory module to coordinate cell proliferation with differentiation in shoot and root.
- 636 *Proceedings of the National Academy of Sciences of the United States of America*
- 637 115(13):e3045-e3054
- 638 Yu L, Chen HW, Hong PP, Wang HL, Liu KF. 2015. Adventitious Bud Induction and Plant
- 639 Regeneration from Stem Nodes of *Salvia splendens* ‘Cailinghong’. *HORTSCIENCE*:869-872
- 640 Yuan JB, Sun XB, Guo T, Chao YH, Han LB. 2020. Global transcriptome analysis of alfalfa
- 641 reveals six key biological processes of senescent leaves. *PeerJ* 8(1):e8426
- 642 Yu KMJ, McKinley B, Rooney WL, Mullet JE. 2021. High planting density induces the expression
- 643 of GA3-oxidase in leaves and GA mediated stem elongation in bioenergy sorghum. *Scientific*
- 644 *Reports* 11(1):46
- 645 Yan Q, Li J, Lu LY, Gao LJ, Lai DW, Yao N, Yi XF, Wu ZY, Lai ZQ, Zhang JY. 2021. Integrated
- 646 analyses of phenotype, phytohormone, and transcriptome to elucidate the mechanism
- 647 governing internode elongation in two contrasting elephant grass (*Cenchrus purpureus*)
- 648 cultivars. *Industrial Crops & Products* (170): 113693
- 649 Yuan R, Zeng XH, Zhao SB, Wu G, Yan XH. 2019. Identification of Candidate Genes Related to
- 650 Stem Development in *Brassica napus* Using RNA-seq. *Plant Molecular Biology Reporter*
- 651 37(4):347-364

- 652 Ziliotto U, Leinauer B, Lauriault LM, Rimi F, Macolino S. 2010. Alfalfa Yield and Morphology
653 of Three Fall-Dormancy Categories Harvested at Two Phenological Stages in a Subtropical
654 Climate. *Agronomy Journal* 102(6):1578-1585
- 655 Zhang H, Liu XQ, Wang XM, Sun M, Song R, Mao PS, Jia SG. 2021. Genome-Wide Identification
656 of GRAS Gene Family and Their Responses to Abiotic Stress in *Medicago sativa*.
657 *International journal of molecular sciences* 22(14):7729
- 658 Zheng XM, Chen YJ, Zhou YF, Shi KK, Hu X, Li DY, Ye HZ, Zhou Y, Wang K. 2021. Full-
659 length annotation with multistrategy RNA-seq uncovers transcriptional regulation of lncRNAs
660 in cotton. *Plant physiology* 185(1):179-195
- 661 Zhao CS, Atsushi H, Shinjiro Y, Kamiya Yuji, Beers EP. 2011. The Arabidopsis Myb genes
662 MYR1 and MYR2 are redundant negative regulators of flowering time under decreased light
663 intensity. *Plant J* 66(3):502-515

Figure 1(on next page)

Phenotypic evaluation of five alfalfa cultivars.

The dynamics of plant height (a), stem diameter (b) and internode length (c) development of five alfalfa cultivars at transplanting stage, b ranching stage , b-udding stage , e-arly flower stage and f-ull flower stage . Average plant height (d), stem diameter (e), internode length (f) of five alfalfa cultivars. The values are the average of fifteen biological replicates and error bars represent the standard deviation. Different letters indicate significant difference at $P < 0.05$ among the five cultivars as determined by Student's test.

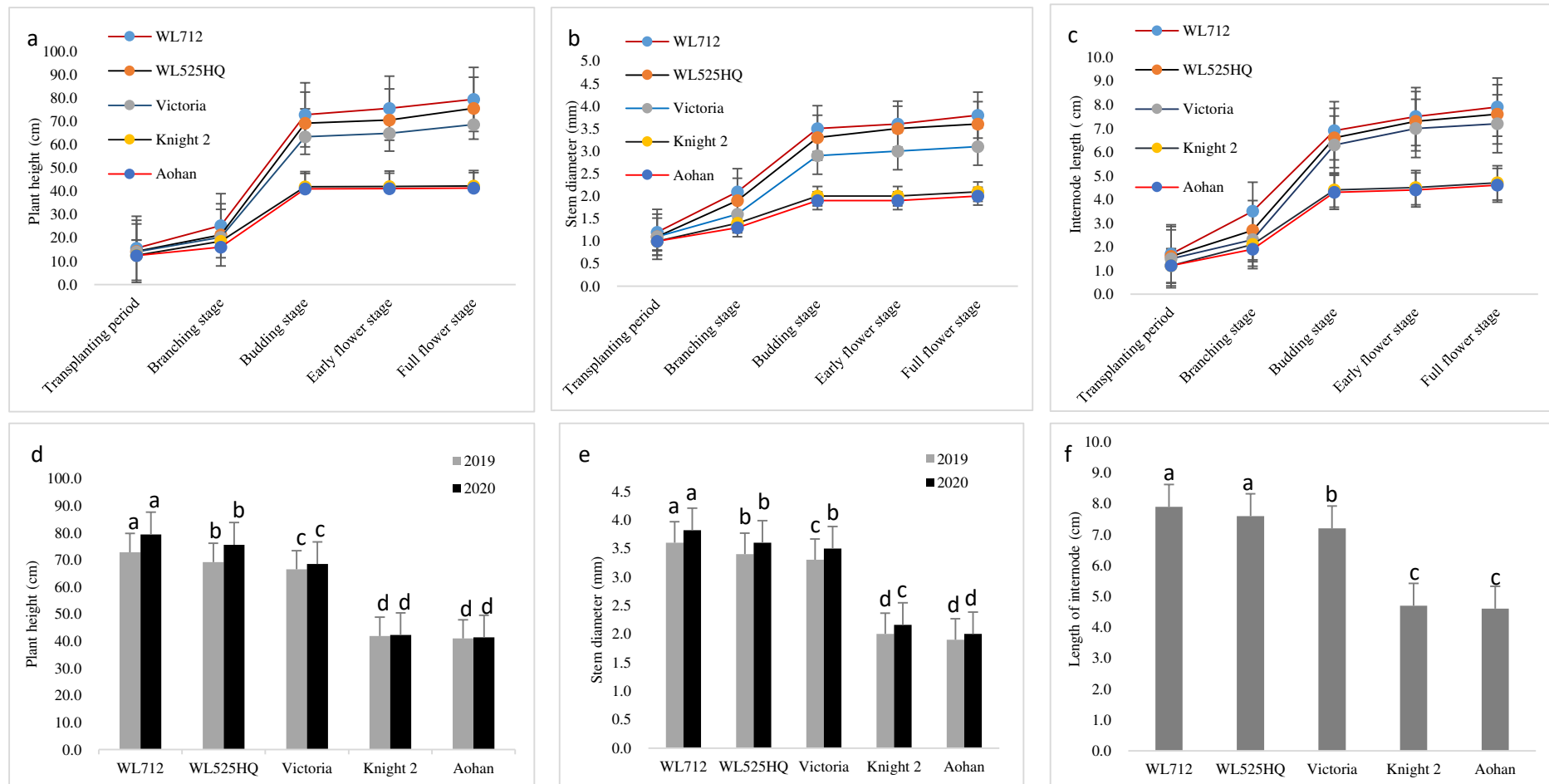


Figure 1 Phenotypic evaluation of five alfalfa cultivars. The dynamics of plant height (a), stem diameter (b) and internode length (c) development of five alfalfa cultivars at transplanting stage, branching stage, budding stage, early flower stage and full flower stage. Average plant height (d), stem diameter (e), internode length (f) of five alfalfa cultivars. The values are the average of fifteen biological replicates and error bars represent the standard deviation. Different letters indicate significant difference at $P < 0.05$ among the five cultivars as determined by Student's test.

Figure 2

Phenotypic evaluation of five alfalfa cultivars

Lateral branches number (a), branches number (b), leaf area (c), fresh weight (d), leaf to stem ratio (e) and dry weight (f) of five alfalfa cultivars. The values are the average of fifteen biological replicates and error bars represent the standard deviation. Different letters indicate significant difference at $P < 0.05$ among the five cultivars as determined by Student's test.

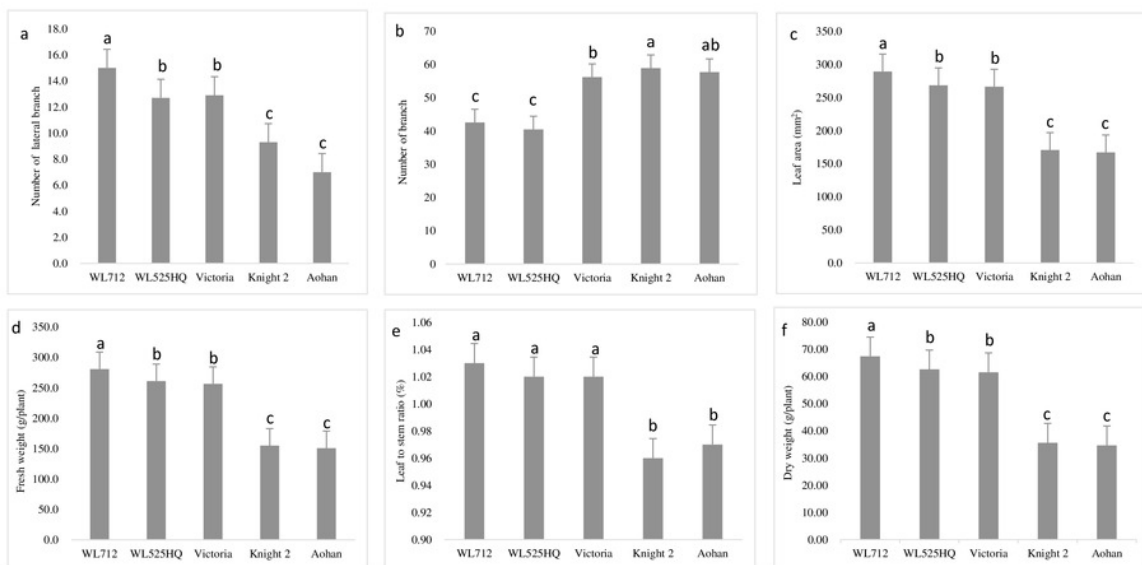


Figure 2 Phenotypic evaluation of five alfalfa cultivars. Lateral branches number (a), branches number (b), leaf area (c), fresh weight (d), leaf to stem ratio (e) and dry weight (f) of five alfalfa cultivars. The values are the average of fifteen biological replicates and error bars represent the standard deviation. Different letters indicate significant difference at $P < 0.05$ among the five cultivars as determined by Student's test.

Figure 3(on next page)

a. Scatter diagram of enriched GO functional. b. KEGG classification of DEGs

a. The “ GeneRatio ” shows the ratio of the number of ~~the~~ DEGs to the total number of differential genes ~~on the GO number~~. b. X axis is the number of gene annotations; Y axis is the type of KEGG pathway.



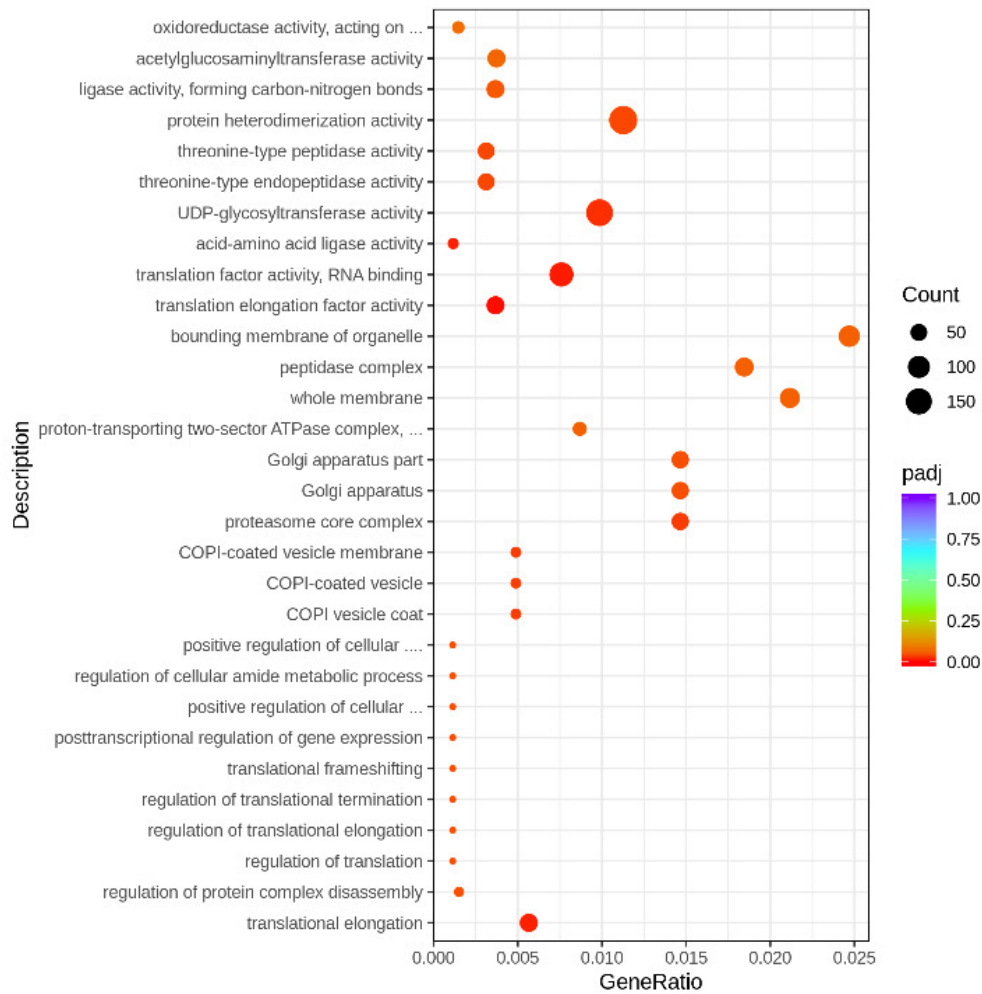


Figure 3a Scatter diagram of enriched GO functional. The “GeneRatio” shows the ratio of the number of the DEGs to the total number of differential genes on the GO number.

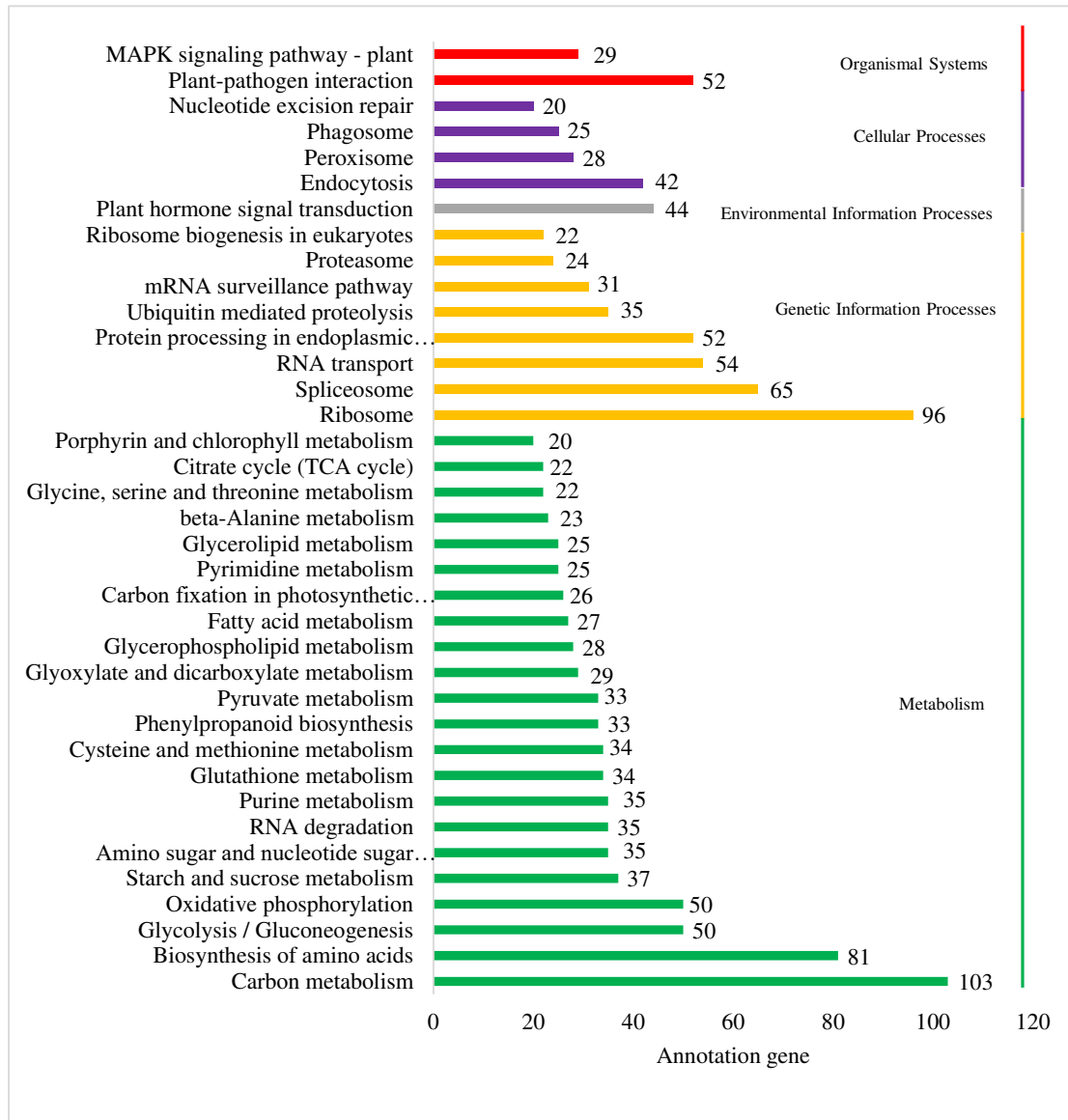
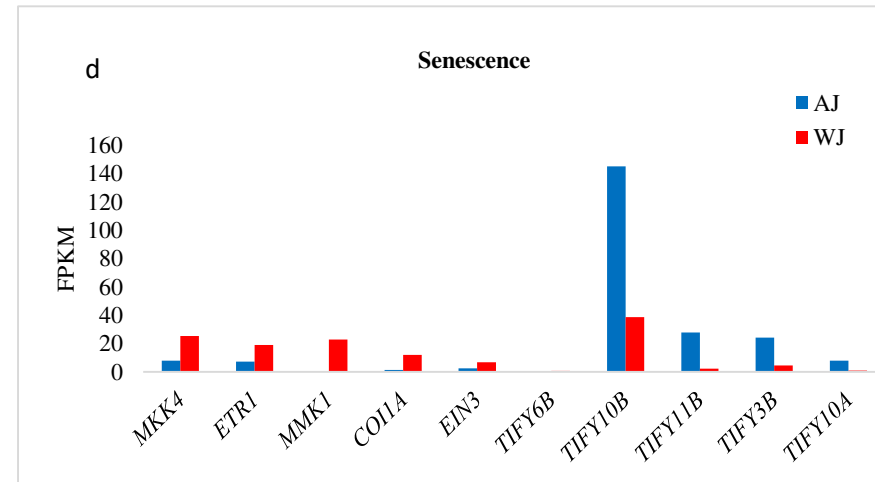
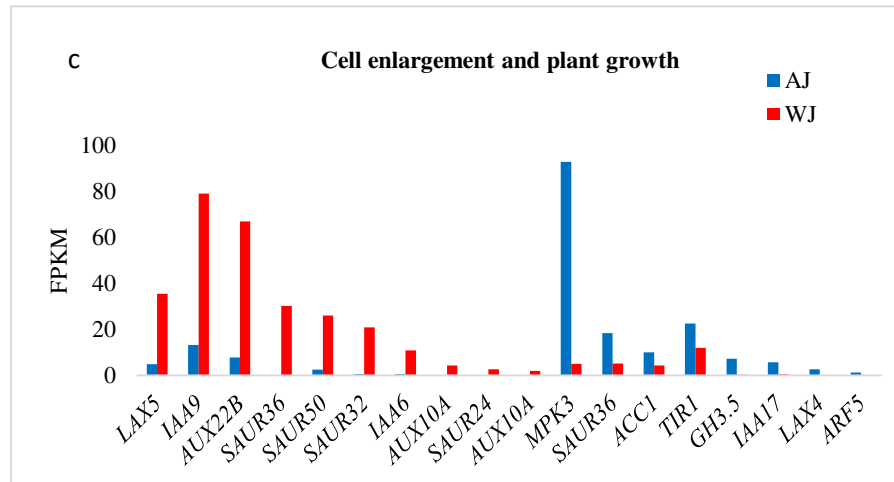
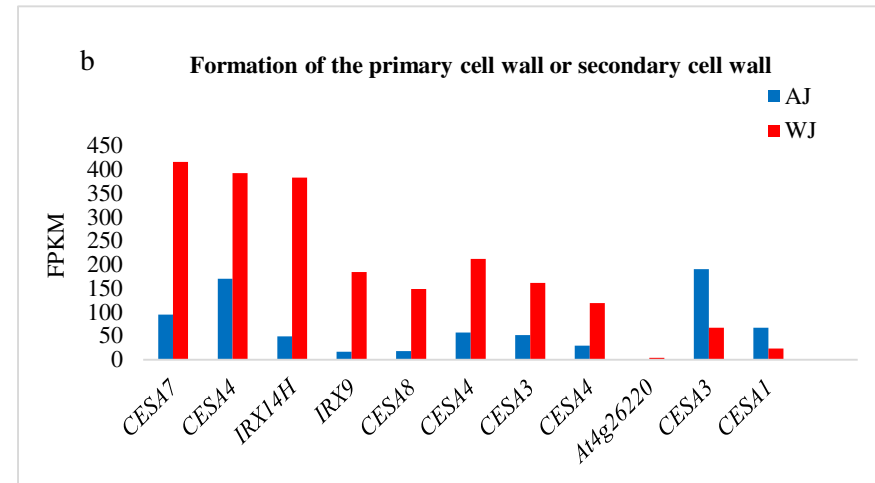
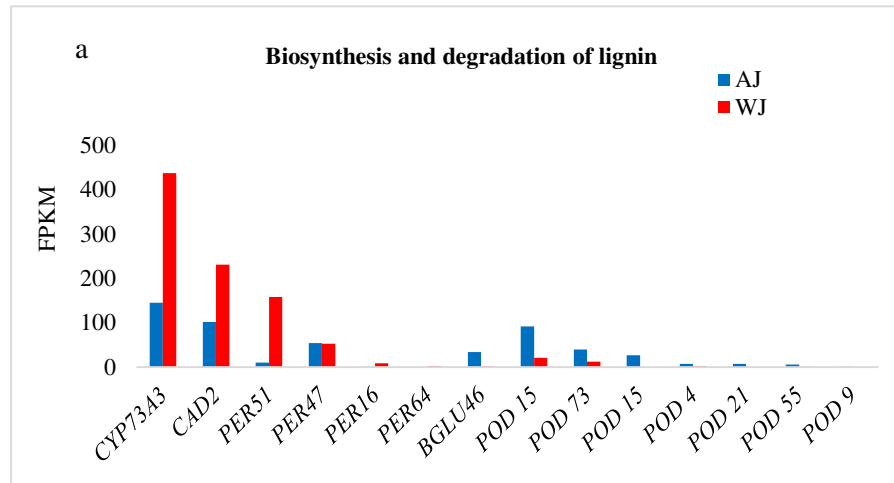


Figure 3b KEGG classification of DEGs; X axis is the number of gene annotations; Y axis is the type of KEGG pathway.

Figure 4(on next page)

The bar graphs showing F PKM of DEGs involved in eight biological processes by GO enrichment analysis.

(a) Biosynthesis and degradation of lignin; (b) Formation of the primary cell wall or secondary cell wall; (c) Cell enlargement and plant growth; (d) Senescence; (e) Cell division and shoot initiation; (f) Stem growth and induced germination; (g) Cell elongation; (h) Formation of water conducting tissues.



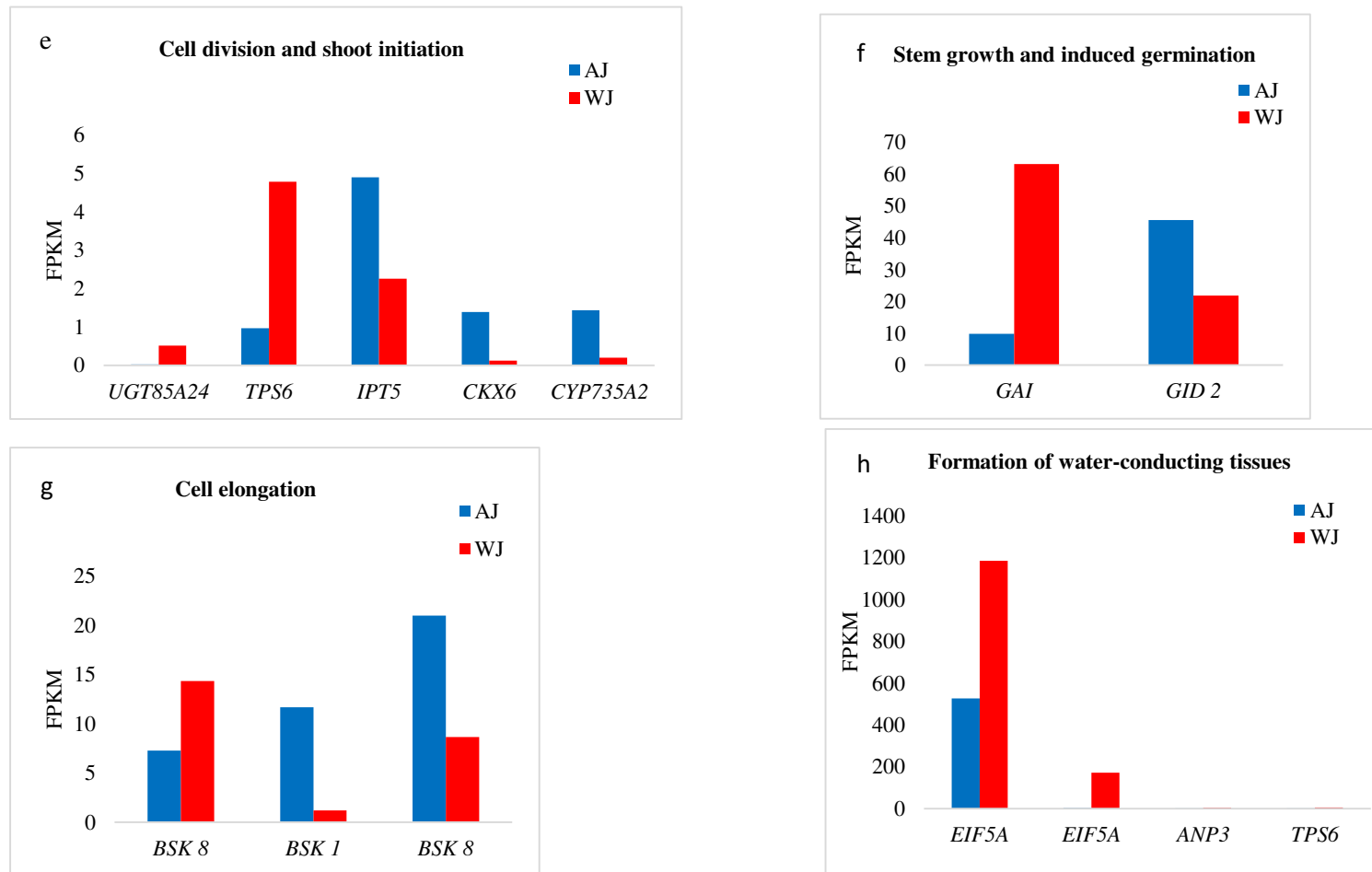


Figure 4 The bar graphs showing FPKM of DEGs involved in eight biological processes by GO enrichment analysis. (a) Biosynthesis and degradation of lignin; (b) Formation of the primary cell wall or secondary cell wall; (c) Cell enlargement and plant growth; (d) Senescence; (e) Cell division and shoot initiation; (f) Stem growth and induced germination; (g) Cell elongation; (h) Formation of water-conducting tissues.

Figure 5

TFs involved in stem elongation and diameter enlargement in alfalfa

(a) Bar graphs shows the FPKM of nine DEGs at different transcriptome databases. Different colors represents different databases including Aohan (AJ) and WL712 (WJ). (b) Histogram shows the nine DEGs relative expression levels of AJ and WJ.

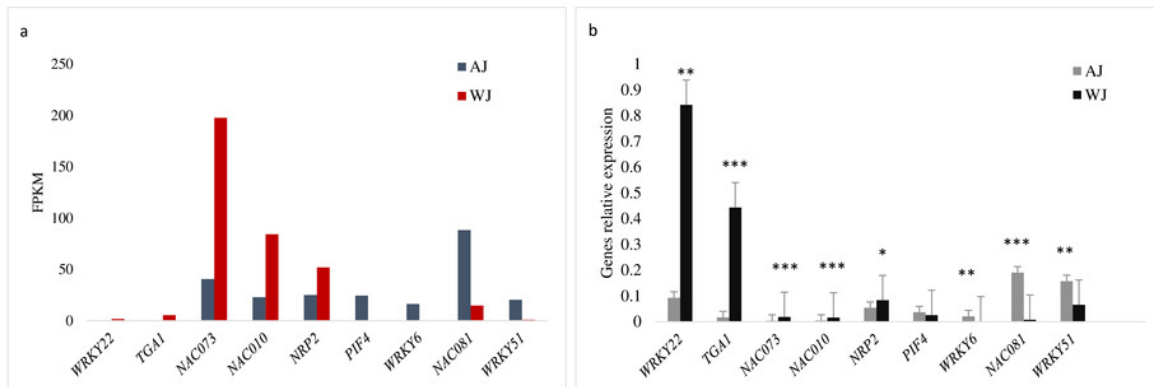


Figure 5 TFs involved in stem elongation and diameter enlargement in alfalfa. (a) Bar graphs shows the FPKM of nine DEGs at different transcriptome databases. Different colors represents different databases including Aohan (AJ) and WL712 (WJ). (b) Histogram shows the nine DEGs relative expression levels of AJ and WJ.

Figure 6

qRT-PCR validation of DEGs from the AJ and WJ RNA-seq databases in alfalfa.

(a) Histogram shows the Fpkm of eleven DEGs at different transcriptome databases. Different colors represents different databases including Aohan (AJ) and WL712 (WJ). (b) Histogram shows the eleven DEGs relative expression levels of AJ and WJ validated by qPCR.

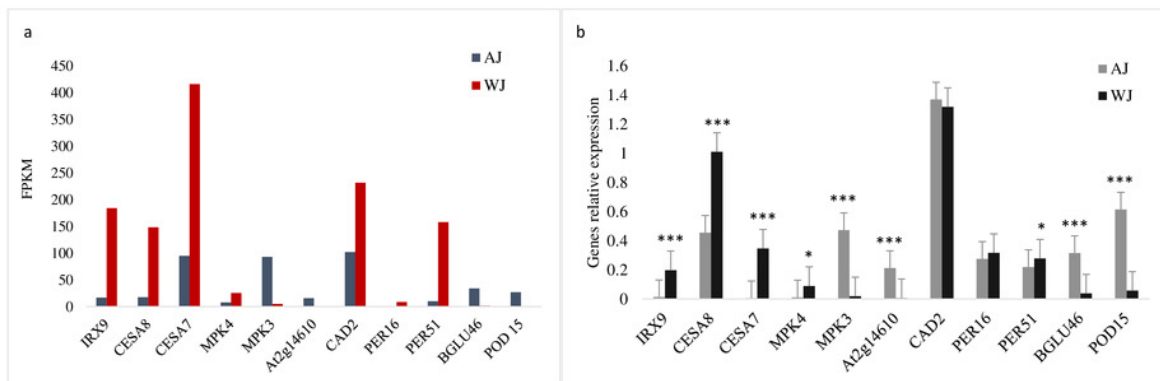


Figure 6 qRT-PCR validation of DEGs from the AJ and WJ RNA-seq databases in alfalfa. (a) Histogram shows the Fpkm of eleven DEGs at different transcriptome databases. Different colors represents different databases including Aohan (AJ) and WL712 (WJ). (b) Histogram shows the eleven DEGs relative expression levels of AJ and WJ validated by qPCR.

Table 1 (on next page)

Phenotypic correlation coefficients between traits based on the five alfalfa cultivars

*, ** Significant at the 0.05, 0.01 ~~and 0.001~~ probability levels, respectively. PH, plant height; IL, internode length; SD, stem diameter; FW, fresh weight; LSR, leaf-to-stem ratio; DW, Dry weight; LBN, lateral branch number; MBN, main branch number.

1 **Table 1.** Phenotypic correlation coefficients between traits based on the five alfalfa cultivars

2

	PH	SD	IL	LBN	MBN	FW	LSR	DW
PH	1							
SD	0.98**	1						
IL	0.99**	0.98**	1					
LBN	0.89**	0.92**	0.90**	1				
MBN	-0.84**	-0.76**	-0.79**	-0.68**	1			
FW	0.98**	0.98**	0.98**	0.91**	-0.75**	1		
LSR	0.55**	0.54**	0.55**	0.51**	-0.46*	0.60**	1	
DW	0.99**	0.99**	0.99**	0.82**	-0.76**	1.00**	0.59**	1

3

4 *, ** Significant at the 0.05, 0.01 and 0.001 probability levels, respectively.

5 PH, plant height; IL, internode length; SD, stem diameter; FW, fresh weight; LSR, leaf-to-stem ratio; DW, Dry weight; LBN,

6 lateral branch number; MBN, main branch number.

Table 2 (on next page)

The growth index of the two varieties in greenhouse

Different letters indicate significant difference at $P < 0.05$ among the two hormones as determined by Student's test

1
2**Table 2 The growth index of the two varieties in greenhouse**

	Plant Height (cm)	Length of Internodde (cm)	Stem Diameter (mm)	Leaf Areas (mm²)	Plant Weight (g/plant)
WL 712	50.16 ± 0.9646 ^a	5.14 ± 0.0911 ^a	2.52 ± 0.0224 ^a	159.38 ± 0.6058 ^a	230.94 ± 2.4450 ^a
Aohan	28.73 ± 0.8027 ^c	2.94 ± 0.0695 ^c	1.19 ± 0.0274 ^c	127.36 ± 2.8085 ^c	141.06 ± 0.4037 ^c

3

4 Different letters indicate significant difference at $P < 0.05$ among the two hormones as determined by Student's test.

Table 3 (on next page)

Top 10 gene ontology function classification

Table 3 Top 10 gene ontology function classification

Category	Description	GO ID	Count	Percentage(%)
Biological process	translational elongation	GO:0006414	41	4.30
	regulation of protein complex disassembly	GO:0043244	8	0.84
	regulation of translation	GO:0006417	7	0.73
	regulation of translational elongation	GO:0006448	7	0.73
	regulation of translational termination	GO:0006449	7	0.73
	translational frameshifting	GO:0006452	7	0.73
	posttranscriptional regulation of gene expression	GO:0010608	7	0.73
	positive regulation of cellular protein metabolic process	GO:0032270	7	0.73
	regulation of cellular amide metabolic process	GO:0034248	7	0.73
	positive regulation of cellular amide metabolic process	GO:0034250	7	0.73
Cell component	bounding membrane of organelle	GO:0098588	57	5.97
	peptidase complex	GO:1905368	44	4.61
	whole membrane	GO:0098805	49	5.13
	proton-transporting two-sector ATPase complex	GO:0033177	20	2.10
	Golgi apparatus part	GO:0044431	36	3.77
	Golgi apparatus	GO:0005794	36	3.77
	proteasome core complex	GO:0005839	37	3.88
	COPI-coated vesicle membrane	GO:0030126	9	0.94
	COPI-coated vesicle	GO:0030137	9	0.94
COPI vesicle coat	GO:0030126	9	0.94	
Molecular function	translation elongation factor activity	GO:0003746	41	4.30
	translation factor activity, RNA binding	GO:0008135	86	9.01
	acid-amino acid ligase activity	GO:0016881	12	1.26
	UDP-glycosyltransferase activity	GO:0008194	99	1.04
	threonine-type endopeptidase activity	GO:0004298	37	3.88
	threonine-type peptidase activity	GO:0070003	37	3.88
	protein heterodimerization activity	GO:0046982	114	11.95
	ligase activity, forming carbon-nitrogen bonds	GO:0016879	35	3.67
	acetylglucosaminyltransferase activity	GO:0008375	35	3.67
oxidoreductase activity	GO:0016638	12	1.26	

3